UV Light Activated SnO_2/ZnO Nanofibers for Gas Sensing at Room Temperature

Jinze Li[1], Ding Gu[1], Yating Yang[1], Haiying Du[2] and Xiaogan Li[1]*

[1] Key Laboratory of Liaoning for Integrated Circuits Technology, School of Microelectronics, Dalian University of Technology, Dalian, China, [2] College of Mechanical and Electronic Engineering, Dalian Minzu University, Dalian, China

Hierarchical SnO_2/ZnO nanofiber heterojunctions composed of SnO_2 nanofiber matrix on top of which ZnO nanorods protruding 30–90 nm long were assembled, were examined for chemiresistive-type gas sensors under UV activation at room temperature. The sensor demonstrated excellent sensitivity to different concentrations of formaldehyde and selectivity to several possible interferents such as alcohols, methanol, benzene, methylbenzene, and acetone with UV LED at a wavelength of 365 nm. The fiber-like heterojunctions can facilitate the electron transfer from ZnO to SnO_2 and this effect would be augmented further under UV light activation. Consequently it enhanced the oxygen adsorptions on the surface of the heterojunctions thus leading to the excellent sensing performance even at room temperature. The influence of the power density and wavelength of UV light used and ambient humidity on the sensor response was systematically investigated. Comparing to the conventional thermal activated one that instead showed preferred response to acetone at 375°C, the enhanced sensitivity and selectivity of the same sensor at room temperature under LED UV light can be attributed to selective photo-catalytic effect induced by the UV light.

Keywords: SnO_2/ZnO nanofiber, heterojunctions, formaldehyde, gas sensor, UV activation

INTRODUCTION

Semiconductor metal oxides (SMO) based chemical gas sensors have been used for detection of the harmful and toxic gases in many fields because of its fast response, high precision, small size, and low cost since it was introduced in 1962 (Seiyama and Kagawa, 1966; Shimizu and Egashira, 1999; Barsan and Weimar, 2001; Yamazoe, 2005; Tiemann, 2007; Lee, 2009; Miller et al., 2014; Liang et al., 2015; Walker et al., 2019). Formaldehyde is one of the most common indoor air pollutant and many furniture materials are the potential source of formaldehyde, which is the allergen of skins and a typical carcinogen (Wood and Coleman, 1995). Therefore, it is significant to develop a reliable sensor to detect the formaldehyde and it is also meaningful for the Internet of Things (IOTs). Nanostructured semiconducting metal oxides such as SnO_2, ZnO, In_2O_5, and TiO_2 have been studied to detect formaldehyde because the nanostructure enhances the interaction with the targeted gas and improves the selectivity and response speed (Seiyama and Kagawa, 1966; Shimizu and Egashira, 1999; Barsan and Weimar, 2001; Yamazoe, 2005; Tiemann, 2007; Lee, 2009; Miller et al., 2014; Liang et al., 2015; Walker et al., 2019). However, the traditional metal oxide based

chemiresistive-type gas sensors often require to work at high temperatures from 200 to 400°C and thus it demands a high electrical power supply (Seiyama and Kagawa, 1966; Shimizu and Egashira, 1999; Barsan and Weimar, 2001; Yamazoe, 2005; Tiemann, 2007; Lee, 2009; Miller et al., 2014; Liang et al., 2015; Walker et al., 2019). Furthermore, it would also have a safety-issue when it is used for detecting flammable gases. Moreover, at the elevated temperature, Metal oxides grain boundaries have an undesirable long-term drift problems caused by the sintering effects.

Recently, an alternative method utilizing the light energy to activate the sensing process of the SMO based gas sensors have been reported extensively (Camagni et al., 1996; Fan et al., 2009; Prades et al., 2009; Lu et al., 2012; Wu et al., 2012; Liu et al., 2013; Park et al., 2013; Zhang et al., 2014; Li et al., 2015, 2017; Chen et al., 2016; Saboor et al., 2016; Gu et al., 2017a). Adopting the light with a wavelength at or close to the corresponding optical forbidden bandgap of the SMO, the sensing properties of SMO based sensors can be significantly enhanced at much lower operating temperature or even room temperature (Camagni et al., 1996; Fan et al., 2009; Prades et al., 2009; Lu et al., 2012; Wu et al., 2012; Liu et al., 2013; Park et al., 2013; Zhang et al., 2014; Li et al., 2015, 2017; Chen et al., 2016; Saboor et al., 2016; Gu et al., 2017a). The photogenerated electrons or holes can facilitate the chemical redox reactions between pre-adsorbed ionized oxygens and the targeted gas molecules thus inducing a sensor signal even at room temperature. Zhang made TiO_2 nanoparticles based chemiresistive gas sensor with the light illumination and working in the condition of 60°C (Zhang et al., 2014). However, by using the hollow structured TiO_2 nanotubes or microspheres, the selectivity and response speeds are improved significantly (Wu et al., 2012; Liu et al., 2013; Li et al., 2015; Chen et al., 2016). Chen et al. (2016) made a hollow ZnO based gas sensor and found a very promising to be used for a selective ethanol sensor working at 80°C with the UV activation. One more benefit of using light activation instead of DC-powered heaters may be that the light can be easily driven up by the random-mechanic vibration energy harvested by using triboelectric nanogenerators as demonstrated recently (Gu et al., 2017a). To facilitate the separation of photogenerated electron/hole pairs thus further improving the sensing performance under light activation, the formed heterojunctions between two or more different SMOs have been studied (Lu et al., 2012; Miller et al., 2014; Gu et al., 2017b; Walker et al., 2019). Lu et al. (2012) reported a NO_2 sensor using SnO_2 nanofibers decorated by ZnO under UV activation. The improved sensitivity was attributed to the formed heterojunctions facilitating the separation of the electron/hole pairs.

In this work, the porous SnO_2 nanofibers with ZnO heterojunctions have been examined for a gas sensor working at room temperatures under UV activation. Compared to its excellent sensitivity but poor selectivity to acetone operated under conventional heating method, the porous SnO_2 nanofiber/ZnO heterojunctions indicated a good sensitivity and selectivity to formaldehyde at room temperature under a UV (365 nm) LED illumination.

EXPERIMENTAL

Materials Preparation and Characterization

The SnO_2/ZnO heterojunction nanofibers were prepared following a two-step process (Mailhiot and Duke, 1986; Du et al., 2018). Firstly, the SnO_2 nanofibers were synthesized by the high-voltage electrospinning method. A certain amount of stannous chloride ($SnCl_2 \cdot 2H_2O$) was added to the ethanol solute and the solution was magnetically stirred for about 1 h until stannous chloride was completely dissolved. Subsequently, the polyvinylpyrrolidone (PVP'MW = 13,000,000) and IV'IV-dimethylformamide (DMF) were added into the mixed solution. The mixture was then stirred magnetically for 3 h at ambient temperature until PVP was completely dissolved to obtain a transparent viscous precursor ready for the followed electrospinning process. The precursor was then injected into
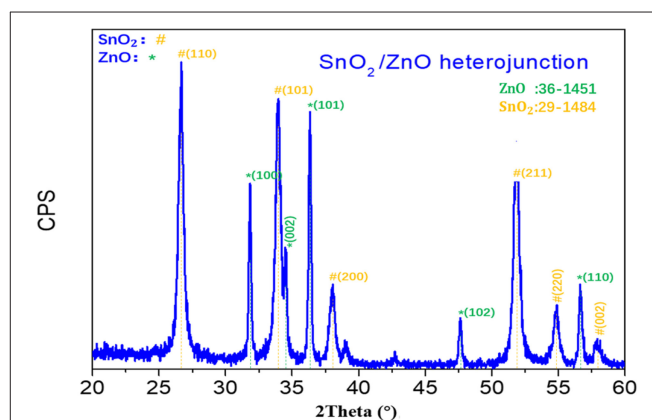

FIGURE 1 | XRD patterns of the SnO_2/ZnO composite heterojunction material.
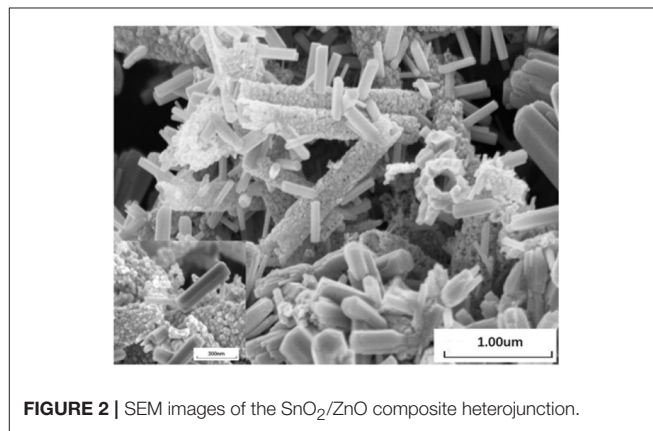

FIGURE 2 | SEM images of the SnO_2/ZnO composite heterojunction.

TABLE 1 | Element contents of SnO_2/ZnO composite heterojunctions.

Elements	wt%
O K	16.6
Zn K	18.9
Sn L	64.5

the electrospinning apparatus. A high-voltage at 20 kV was applied across the collecting plate and the nozzle with a distance of 13 cm in between. During the electrospinning process, the precursor was squeezed through the needle-like nozzle and the electro-spun nanofibers were collected on the collecting plate. Then, the collected white nanofibers were calcined at 600 °C for 2 h to obtain the SnO_2 nanofiber framework. For a comparison, tin oxide nanoparticles were prepared by using the similar process with the replacement of PVP by PMMA in the electrospinning precursor.

Secondly, the SnO_2 nanofibers heterojuncted with the secondary phase of ZnO nanoparticles were prepared. A certain amount of SnO_2 nanofibers as obtained earlier was mixed with deionized water and the slurry was ground into a paste in an agate mortar. Then, the paste was spinning-coated onto a glass substrate and a drop of 0.05 mol/L zinc acetate in ethanol solution was evenly spread over the glass substrate. The substrate was baked in an oven at 200 °C for half an hour to grow the ZnO seeds on the SnO_2 nanofiber framework. Subsequently, the baked glass substrate was immersed into a solution of 0.04 mol/L zinc acetate in ethanol in a vessel and the whole set was heated in water bath at a constant temperature of 90 °C for 4 h to fabricate the final SnO_2/ZnO heterojunction product. After drying at room temperature, a white powdered SnO_2/ZnO heterogeneous composite was obtained.

The powder X-ray diffraction patterns (XRD) of the samples were characterized by an X-ray diffractometer (XRD-6000, Shimadzu Corp.), utilizing the Cu-Ka radiation at 40 kV and 30 mA. The surface morphology of the heterojunction samples was characterized by the Scanning Electron Microscope (SEM: S-3000N, Hitachi, Japan). The X-ray photoelectron spectroscopy (XPS) was recorded by a Thermo ESCALAB 250 Xi X-ray photoelectron spectroscopy using an Al radiation excitation source operating at 150 W and a beam spot size of 500 μm while the binding energy was calibrated by C1s at 284.8 eV.

## Sensor Fabrication and Electrical Measurements

The chemical resistance sensor was fabricated by depositing the SnO_2/ZnO composite heterojunctions on an alumina substrate

preliminarily printed with the gold electrodes at a spacing distance around 200 μm.

During the sensing measurements, the LED light sources at three different wavelengths (365 nm, 395 nm, 405 nm) were placed, respectively, above the sensor to provide the activation energy to the sensor. Before the testing, the sensors were illuminated under the LED light for 10 min to reach a stable state of the resistance. The distance between LED light and the sensor is 1 cm and the sensors were operated at the room temperature (25 °C). The gas sensing characteristics of the sensor was tested in a sealed chamber with an inner volume of 50 L. The relative humidity in the chamber is measured by a hydrometer. The different concentrations of the testing gases were achieved by evaporation of the corresponding liquids. The resistances of the sensors were measured for the sensor signals by the multimeter (Agilent 34410A) automatically controlled by a PC. The response of sensor (R_s) is defined by the relative change of the sensor resistance in air (R_a) and in test gas (R_s) according
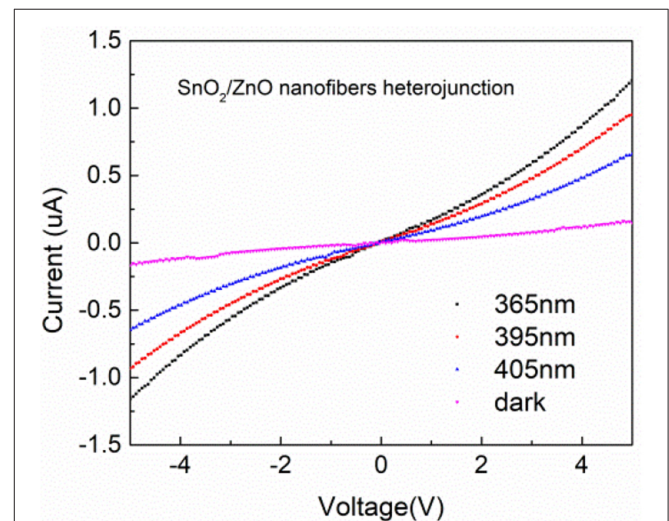
FIGURE 4 | I–V polarization curves of the SnO_2/ZnO composite heterojunction material under different light sources.
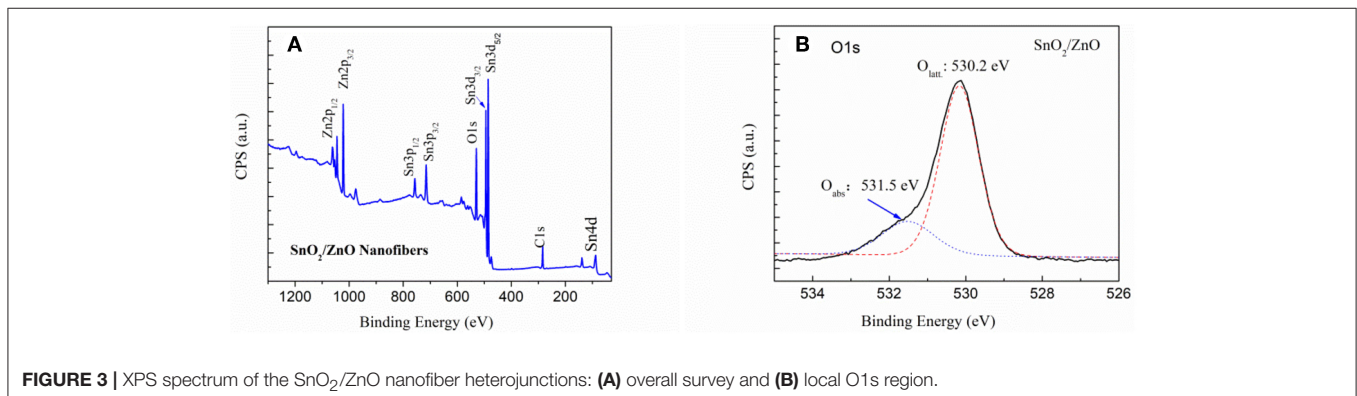
FIGURE 3 | XPS spectrum of the SnO_2/ZnO nanofiber heterojunctions: **(A)** overall survey and **(B)** local O1s region.

to below equation:

$$R_s = \frac{R_a}{R_g} \ (for \ reducing - type \ gas)$$

RESULTS AND DISCUSSION

Microstructure Characterization

Figure 1 shows the XRD pattern of the fabricated SnO_2/ZnO composite heterojunction material. It shows that the SnO_2/ZnO heterojunction has both a tetragonal rutile structure of SnO_2 and a hexagonal wurtzite structure of ZnO which are indexed according to JCPDS No.41-1445 and 36-1451, respectively. There is no other impure phase, indicating that there is no chemical reaction between SnO_2 nanofibers and ZnO nanoparticles formed on the nanofibers during the thermal treatments.
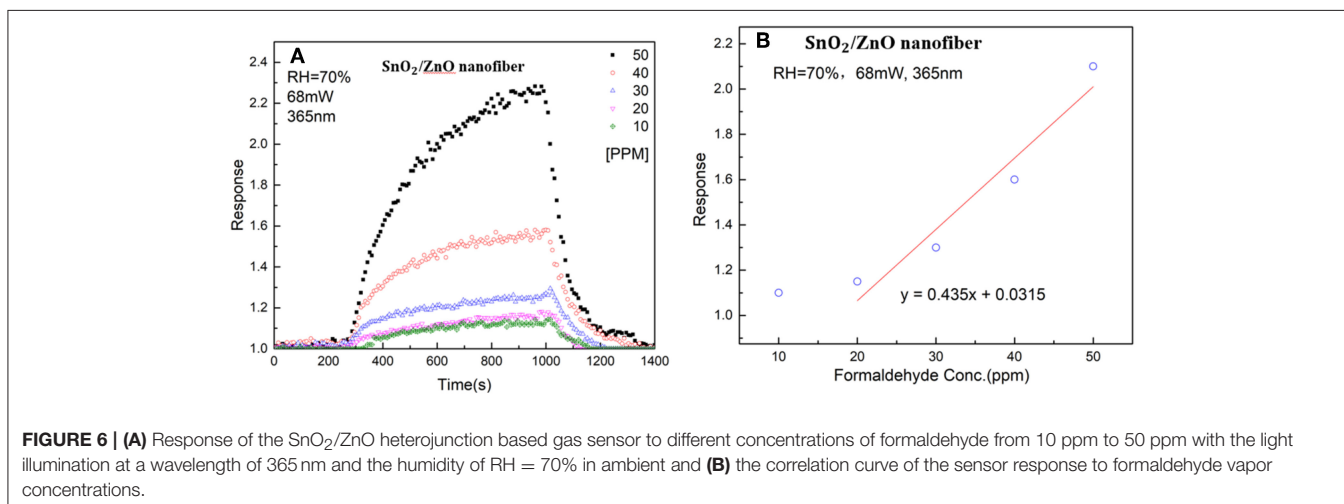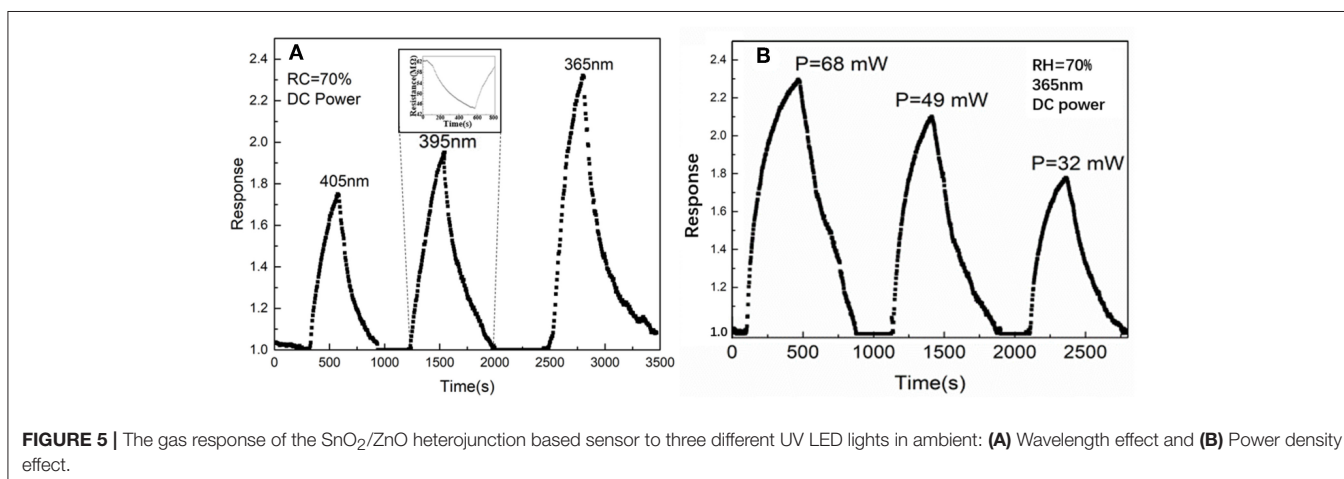
Figure 2 shows the SEM images of the SnO_2/ZnO composite heterojunction material. The SEM image indicate the SnO_2 nanofibers the porous microstructure. It is obvious that ellipsoid ZnO nanoparticles were grown on the nanofiber structure of SnO_2. The diameter of the SnO_2 nanofiber is about 300 nm. The diameter of the ZnO nanoparticles is about 30~90 nm. **Table 1**

lists the content of each element in the SnO_2/ZnO nanofiber. As shown in the table, the mass ratio of SnO_2 to ZnO is estimated to be approximately 7:2.

Figure 3 shows the XPS spectrum of the SnO_2/ZnO composite heterojunction. **Figure 3A** is the survey of the sample and indicated that there are eight characteristic peaks. The binding energy for the C_{1s} peak at 284.6 eV is used as a reference to calibrate the spectra. **Figure 3B** shows the local region of the O_{1s} in the SnO_2/ZnO composite heterojunction material. The binding energy of O_{1s} at 530.2 eV can be assigned to the lattice oxygen. The lattice oxygen did not participate in the sensing reaction. The O_{ads} is a kind of adsorbed, ionized oxygen usually in the form of O_2^- at low temperatures on the surface of the heterojunction material (Barsan and Weimar, 2001).

Photo-Electronic Characterization and Gas Sensing Performance

The I–V polarization curves of the SnO_2/ZnO composite heterojunction material under different light sources are shown in **Figure 4**. Under UV lights with a wavelength from 405 nm to 365 nm, the measured currents were significantly enhanced

FIGURE 5 | The gas response of the SnO_2/ZnO heterojunction based sensor to three different UV LED lights in ambient: **(A)** Wavelength effect and **(B)** Power density effect.

FIGURE 6 | (A) Response of the SnO_2/ZnO heterojunction based gas sensor to different concentrations of formaldehyde from 10 ppm to 50 ppm with the light illumination at a wavelength of 365 nm and the humidity of RH = 70% in ambient and **(B)** the correlation curve of the sensor response to formaldehyde vapor concentrations.

compared to the dark and increased as the wavelength became shorter. There is a slightly non-linear relationship between the measured currents and the applied bias when the applied voltages beyond the range of +4 V to −4 V indicating a non-Ohmic type connections. This is most likely due to the heterojunction formed by the SnO_2 and ZnO which formed the n-n diode junctions indicating slight rectifying properties.

The gas response of the SnO_2/ZnO composite heterojunctions under different wavelength and power density are shown in **Figure 5**. From **Figure 5A**, it can observe that with the shorter wavelength at 365 nm at the same power density, the sensor shows a highest response. This is due to the fact that both SnO_2 and ZnO have a wide-band gap which corresponds to optical wavelength around 360–370 nm depending upon the microstructure and the degree of defective density (Mailhiot and Duke, 1986). Further, **Figure 5B** shows the response of the sensor increased as the power density of the UV light at 365 nm

increased. With the light illumination of 365 nm, the response of SnO_2/ZnO composite heterojunction based sensor rises from 40 to 70% with the power supply increased form 32 mW to 68 mW. However, the response and recovery speeds are sluggish which is mainly due to the slow adsorption and desorption of ionized oxygen during the "on" and "off" states of the sensor.
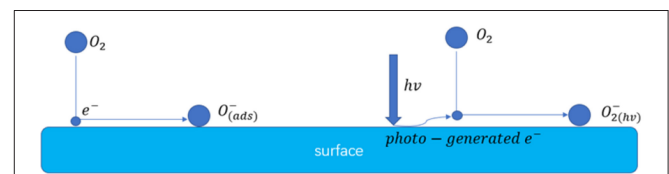
Figure 6A shows the response of the SnO_2/ZnO composite nanofiber heterojunctions based chemiresistive-type sensor to different concentrations of formaldehyde from 10 ppm to 50 ppm with the LED light illumination at the wavelength of 365 nm and at room temperature and the relative humidity of RH = 70% in ambient. It can be observed that with the formaldehyde induced into the testing chamber, the resistance of the sensor reduced and the resistance recover fully back with the formaldehyde vapor was removed from the chamber. It indicates that the SnO_2/ZnO
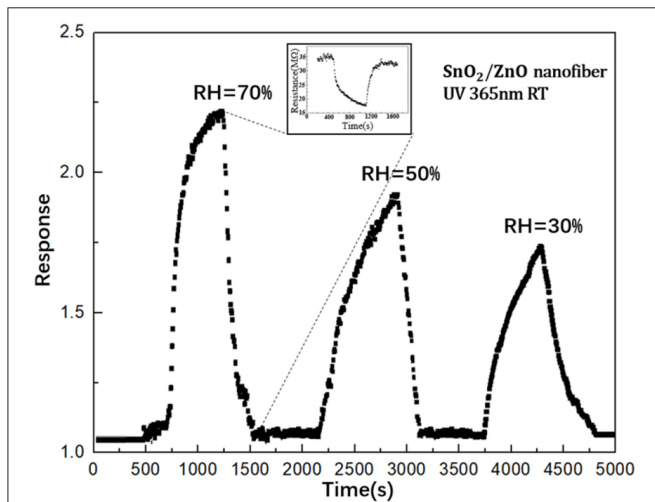

FIGURE 7 | The influence of humidity to the response of SnO_2 based sensor with the light illumination (365 nm) to the 50 ppm formaldehyde.

TABLE 2 | Comparison of the gas sensing properties of SnO_2 based heterojunctions.

Sensing material	Test gas	Irradiation/ T(°C)	Response/ C (ppm)	References
SnO2-ZnO composite film	Ethanol	300°C	4.69/200	Kim et al., 2007
SnO2-ZnO	methanol	350°C	8.5/10	Yan et al., 2015
SnO2-ZnO	o_2	UV/R.T.	2.25/250	Xiong et al., 2017
SnO2-ZnO	CO	UV/R.T.	0.12/250	Camagni et al., 1996
SnO2/ZnO	HCHO	UV/R.T.	2.3/50	This work

FIGURE 9 | Schematic illustration of possible enhanced gas sensing mechanism of the sensors under 365 nm light activation.
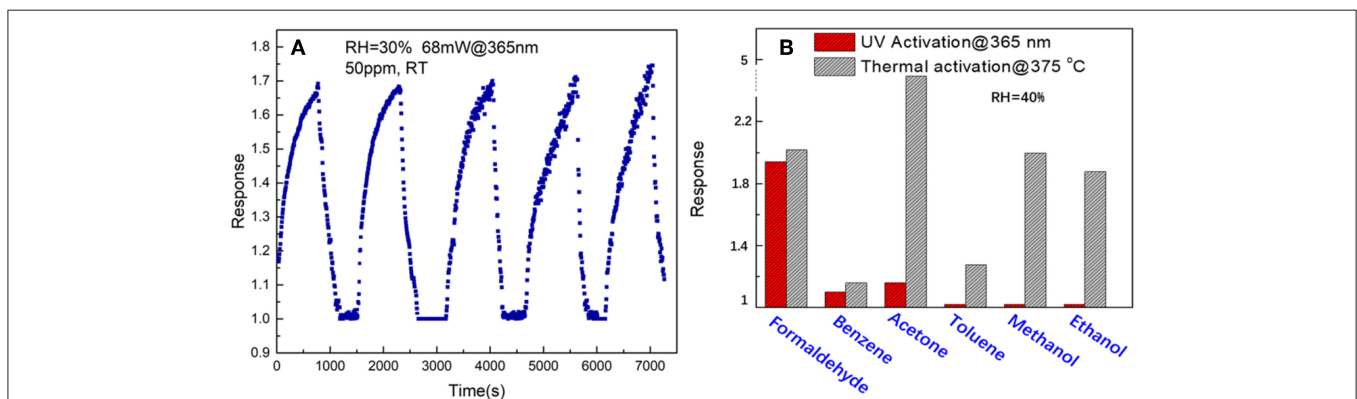
FIGURE 8 | (A) Signal repeatability and **(B)** comparison of the response of the SnO_2/ZnO heterojunction based sensor to formaldehyde with other several possible interference such as benzene, acetone, toluene, methanol and ethanol with 50 ppm each under the 365 nm light illumination and with the humidity of RH=40%.

heterojunction shows a typical n-type response behavior since the formaldehyde is regarded as a reducing-type gas and would consume the adsorbed ionized oxygen thus releasing the trapped electrons back to the sensing materials. As the concentrations of the formaldehyde increased from 10 ppm to 50 ppm, the sensor response increased from 10 to 70 %. **Figure 6B** shows the relationship between the sensor response and the formaldehyde concentrations indicates a non-linear feature. Moreover, as the concentrations of formaldehyde increased, the response and recovery times increased too. This may be because as the number of the testing gas molecules in the air increased, it consumed more time to react with the adsorbed ionized oxygen on the surface of the heterojunctions.

Figure 7 shows the influence of humidity to the response of SnO_2/ZnO composite heterojunction based formaldehyde sensor with the UV light activation (365 nm) to the 50 ppm formaldehyde at room temperature. It can observe that with the increase of the relative humidity in testing chamber from 30 to 70 %, the response of the sensor increased. This is contrary to the response of the most SMO based chemiresistive-type gas sensors when operated at the conventional heating model, during which the response would be significantly suppressed when the relative humidity increased. Here, it could be due to the assistance of the adsorbed H_2O molecule in the photocatalytic oxidation of formaldehyde by the pre-adsorbed ionized oxygen (Liu et al., 2013).

Figure 8A shows the repeatability of response curves of the SnO_2/ZnO composite heterojunction based sensor to 50 ppm formaldehyde under the 365 nm light illumination at 25°C with the relative humidity of 30%. The sensor shows an excellent signal repeatability and stable response at 25°C when periodically exposed to the formaldehyde vapor. **Figure 8B** shows the comparison of response of the SnO_2/ZnO nanofiber-shaped composite heterojunction based chemiresistive-type sensor to several possible interferents such as ammonia, benzene, acetone, toluene, methanol and ethanol with 50 ppm each under UV activation and conventional thermal activation at its optimum temperature of 375°C. It indicates that the nanofiber structure of SnO_2/ZnO composite heterojunction based sensor has a much better response to formaldehyde indicating a possible excellent selectivity under UV activation. However, the sensor shows

highest response to acetone instead under thermal activation at 375 °C and also a poor selectivity. It indicates that UV activated SnO_2/ZnO nanofiber heterojunction based sensor could be an effective way to improve the selectivity of the sensor and lower down the operating temperature as well.

The gas properties of SnO_2 based heterojunctions based sensors developed in this work and the previously published data are compared in **Table 2**. It can be observed that SnO_2/ZnO under UV-light irradiation has a good gas-sensing performance to formaldehyde at room temperature.

Sensing Mechanism

At lower operating temperatures below 100°C, the major form of the adsorbed ionized oxygen is O_2^- by trapping the electrons at the surface of the sensing materials according to below possible reaction:

$$O_{2\,(air)} + e^-_{(cond.\ band)} \rightarrow\ 2O^-_{2(ads.)} \tag{1}$$
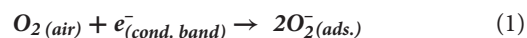
The reason for the induced change of the electrical resistance of the metal oxide based sensors when exposed to the targeted gases is attributed to the redox reactions between these adsorbed ionized oxygen and the targeted gases during which the trapped electrons by oxygen were released back to the sensing materials (Wu et al., 2012; Liu et al., 2013; Li et al., 2015; Chen et al., 2016). However, this sensing reaction process needs higher energy to be triggered at low temperatures.

Figure 9 shows the schematic illustration of the possible enhanced gas sensing mechanism of the sensors under 365 nm light activation. After introducing the UV light energy, the photo-generated electrons reacted with the oxygen in the air and generate O_2^- (hv). When the SnO_2/ZnO composite heterojunction material was exposed to the formaldehyde, the formaldehyde molecules would react with the O_2^- (hv) adsorbed on the surface according to below reaction:

$$HCHO + \ O^-_{2(hv)} \rightarrow\ H_2O + CO_2 + e^- \tag{2}$$
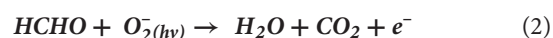
Then, the electrons were released, resulting to the decrease in the resistance of the sensor. However, since the ionized oxygen species with negative monovalence which usually has a lower
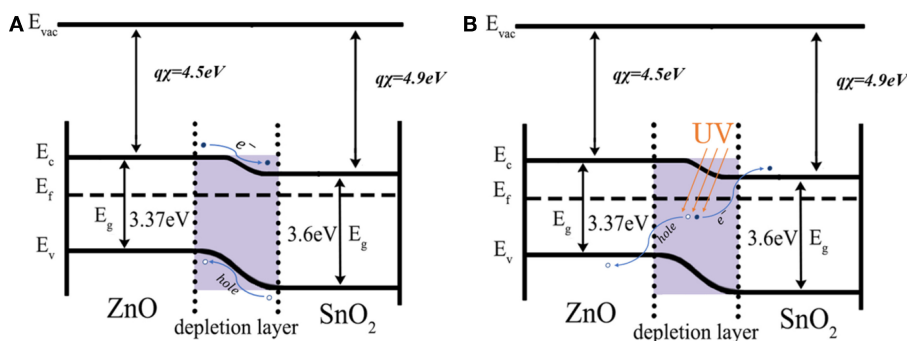
FIGURE 10 | Electron transfer between the formed SnO_2/ZnO nanofiber heterojunctions **(A)** in dark and **(B)** under UV.

photocatalytic properties to react to organic vapors, the reaction of O_2^- according to equation (2) would prefer to react with more active polar gases such as formaldehyde and reluctant to react with the slight inertia gases such as benzene, acetone, ethanol, methanol and toluene thus significantly improving the selectivity of the sensor (Wu et al., 2012; Liu et al., 2013; Li et al., 2015; Chen et al., 2016).

Figure 10 shows a comparison of the band diagrams of ZnO/SnO$_2$ heterojunction under UV light. With the formed heterojunctions between n-type SnO$_2$ and n-type ZnO, the separation of the photogenerated electron/hole pairs can thus be enhanced according to the illustrations shown in **Figure 10**. The electron affinity of tin dioxide and zinc oxide is 4.5 and 4.3 eV, respectively. The work functions of SnO$_2$ and ZnO are 4.9 and 4.45 eV, respectively. The forbidden band gaps of SnO$_2$ and ZnO are 3.6 and 3.37 eV, respectively. Therefore, electrons will transfer from the conduction band of ZnO to that of SnO$_2$ due to the former has a higher energy level of the conduction band when ZnO/SnO$_2$ heterojunctions were formed. With UV light activation, the photogenerated electrons would be extracted to the conduction band of SnO$_2$ and thus there would be more ionized O_2^- according to reaction (1). Consequently, the energy barrier of SnO$_2$/ZnO heterojunctions could reduce the recombination of photogenerated electron/hole pairs making the electrons and holes have a longer remaining lifetime in the sensing materials which thus enhanced the redox reaction according to equation (2) (Lu et al., 2012; Miller et al., 2014; Walker et al., 2019).

CONCLUSIONS

As an alternative method to activate the SMO based chemiresistive-type gas sensors, UV light has been employed to activate the gas sensing properties of the SnO$_2$/ZnO nanofiber heterojunction based chemical gas sensors at room temperature. The SnO$_2$/ZnO nanofiber heterojunctions based sensor shows a good sensitivity to different concentrations of formaldehyde and an excellent selectivity compared to several possible interferents such as ethanol, methanol, acetone, benzene, and toluene under UV at room temperature. The satisfied performance including the sensitivity and selectivity under UV at room temperature could be due to the UV-assisted redox reactions between the polar formaldehyde and the adsorbed, slight-weak oxidant of adsorbed ionized oxygen with monovalence. The formed heterojunctions between SnO$_2$/ZnO can enhance the effective separation of the photogenerated electron/hole pairs making them stay a longer lifetime in the sensing materials. This would further enhance the redox reactions and thus improve the sensitivity of the sensor.

DATA AVAILABILITY

The raw data supporting the conclusions of this manuscript will be made available by the authors, without undue reservation, to any qualified researcher.

AUTHOR CONTRIBUTIONS

JL and DG designed and conducted the study, contributed to the data analysis, and writing the manuscript. YY and HD contributed to data analysis. XL supervised the study and contributed to study design, data analysis and writing the manuscript. All authors provided feedback on the manuscript.

ACKNOWLEDGMENTS

REFERENCES

Barsan, N., and Weimar, U. (2001). Conduction model of metal oxide gas sensors. *J. Electroceram.* 7, 143–167. doi: 10.1023/a:1014405811371

Camagni, P., Faglia, G., Galinetto, P., Perego, C., Samoggia, G., and Sberveglieri, G. (1996). Photosensitivity activation of SnO$_2$ thin film gas sensors at room temperature. *Sens. Actuators B Chem.* 31, 99–103. doi: 10.1016/0925-4005(96)80023-2

Chen, Y., Li, X., Li, X., Wang, J., and Tang, Z. (2016). UV activated hollow ZnO microspheres for selective ethanol sensors at low temperatures. *Sens. Actuators B Chem.* 232, 158–164. doi: 10.1016/j.snb.2016.03.138

Du, H., Li, X., Yao, P., Wang, J., Sun, Y., and Dong, L. (2018). Zinc oxide coated tin oxide nanofibers for improved selective acetone sensing. *Nanomaterials* 8:509. doi: 10.3390/nano8070509

Fan, S. W., Srivastava, A. K., and Dravid, V. P. (2009). UV-activated room-temperature gas sensing mechanism of polycrystalline ZnO. *Appl. Phys. Lett.* 95:142106. doi: 10.1063/1.3243458

Gu, D., Li, X., Wang, H., Li, M., Xi, Y., Chen, Y., et al. (2017a). Light enhanced VOCs sensing of WS$_2$ microflakes based chemiresistive sensors powered by triboelectronic nangenerators. *Sens. Actuators B Chem.* 256, 992–1000. doi: 10.1016/j.snb.2017.10.045

Gu, D., Li, X., Zhao, Y., and Wang, J. (2017b). Enhanced NO$_2$ sensing of SnO$_2$/SnS$_2$ heterojunction based sensor. *Sens. Actuators B Chem.* 244, 67–76. doi: 10.1016/j.snb.2016.12.125

Kim, K. W., Cho, P. S., Kim, S. J., Lee, J. H., Kang, C. Y., and Kim, J. S. (2007). The selective detection of C2H5OH using SnO2–ZnO thin film gas sensors prepared by combinatorial solution deposition. *Sens. Actuators B: Chem.* 123, 318–324. doi: 10.1016/j.snb.2006.08.028

Lee, J. H. (2009). Gas sensors using hierarchical and hollow oxide nanostructures: overview. *Sens. Actuators B Chem.* 140, 319–336. doi: 10.1016/j.snb.2009.04.026

Li, H. Y., Yoon, J. W., Lee, C. S., Lim, K., Yoon J. W., Lee, J. H, et al. (2017). Visible light assisted NO$_2$, sensing at room temperature by CdS nanoflake array. *Sens. Actuators B Chem.* 225, 2963–2970. doi: 10.1016/j.snb.2017.09.118

Li, X., Li, X., Wang, J., and Lin, S. (2015). Highly sensitive and selective room-temperature formaldehyde sensors using hollow TiO$_2$ microspheres. *Sens. Actuators B Chem.* 219, 158–163. doi: 10.1016/j.snb.2015.05.031

Liang, X., Kim, T. H., Yoon, J. W., Kwak, C. H., and Lee, J. H. (2015). Ultrasensitive and ultraselective detection of H$_2$S using electrospun CuO-loaded In$_2$O$_3$ nanofiber sensors assisted by pulse heating. *Sens. Actuators B Chem.* 209, 934–942. doi: 10.1016/j.snb.2014.11.130

Liu, L., Li, X., Dutta, P. K., and Wang, J. (2013). Room temperature impedance spectroscopy-based sensing of formaldehyde with porous TiO$_2$ under UV illumination. *Sens. Actuators B Chem.* 185, 1–9. doi: 10.1016/j.snb.2013.04.090

Lu, G., Xu, J., Sun, J., Yu, Y., Zhang, Y., and Liu, F. (2012). UV-enhanced room temperature NO$_2$ sensor using ZnO nanorods modified with SnO2 nanoparticles. *Sens. Actuators B Chem.* 162, 82–88. doi: 10.1016/j.snb.2011.12.039

Mailhiot, C., and Duke, C. B. (1986). Many-electron model of equilibrium metal-semiconductor contacts and semiconductor heterojunctions. *Phys. Rev. B.* 33, 1118–1133. doi: 10.1103/PhysRevB.33.1118

Miller, D. R., Akbar, S. A., and Morris, P. A. (2014). Nanoscale metal oxide-based heterojunctions for gas sensing: a review. *Sens. Actuators B Chem.* 204, 250–272. doi: 10.1016/j.snb.2014.07.074

Park, S., An, S., Mun, Y., and Lee, C. (2013). UV-enhanced NO$_2$ gas sensing properties of SnO$_2$-Core/ZnO-shell nanowires at room temperature. *ACS Appl. Mater. Interfaces* 5, 4285–4292. doi: 10.1021/am400500a

Prades, J. D., Jimenez-Diaz, R., Manzanares, M., Ramirez, F. H., Cirera, A., Rodriguez, A. R., et al. (2009). A model for the response towards oxidizing gases of photoactivated sensors based on individual SnO$_2$ nanowires. *Phy. Chem. Chem. Phys.* 11:10881. doi: 10.1039/b915646a

Saboor, F. H., Ueda, T., Kamada, K., Hyodo, T., Mortazavi, Y., Khodadadi, A. A., et al. (2016). Enhanced NO$_2$ gas sensing performance of bare and Pd-loaded SnO$_2$ thick film sensors under UV-light irradiation at room temperature. *Sens. Actuators B Chem.* 223, 429–439. doi: 10.1016/j.snb.2015.09.075

Seiyama, T., and Kagawa, S. (1966). Study on a detector for gaseous components using semiconductive thin films. *Analyt. Chem.* 38, 1069–1073. doi: 10.1021/ac60240a031

Shimizu, Y., and Egashira, M. (1999). Basic aspects and challenges of semiconductor gas sensors. *MRS Bull.* 24, 18–24. doi: 10.1557/S0883769400052465.

Tiemann, M. (2007). Porous metal oxides as gas sensors. *Chem. Eur. J.* 13, 8376–8388. doi: 10.1002/chem.200700927

Walker, J. M., Akbar, S. A., and Morris, P. A. (2019). Synergistic effects in gas sensing semiconducting oxide nano-heterostructures: a review. *Sens. Actuators B.* 286, 624–640. doi: 10.1016/j.snb.2019.01.049

Wood, R. W., and Coleman, J. B. (1995). Behavioral evaluation of the irritant properties of formaldehyde. *Tox. Appl. Pharmacol.* 130, 67–72. doi: 10.1006/taap.1995.1009

Wu, G., Zhang, J., Wang, X., Liao, J., Xia, H., Akbar, S. A., et al. (2012). Hierarchical structured TiO$_2$ nanotubes for formaldehyde sensing. *Ceram. Int.* 38, 6341–6347. doi: 10.1016/j.ceramint.2012.05.004

Xiong, Y., Lu, W., Ding, D., Zhu, L., Li, X., Ling, X., and Xue, Q. (2017). Enhanced room temperature oxygen sensing properties of laocl–sno2 hollow spheres by uv light illumination. *ACS Sens.* 2, 679–686. doi: 10.1021/acssensors.7b00129

Yamazoe, N. (2005). Toward innovations of gas sensor technology. *Sens. Actuators B Chem.* 108, 2–14. doi: 10.1016/j.snb.2004.12.075

Yan, S. H., Ma, S. Y., Li, W. Q., Xu, X. L., Cheng, L., Song, H. S., et al. (2015). Synthesis of SnO2–ZnO heterostructured nanofibers for enhanced ethanol gas-sensing performance. *Sens. Actuators B Chem.* 221, 88–95. doi: 10.1016/j.snb.2015.06.104

Zhang, S., Lei, T., Li, D., Zhang, G., and Xie, C. (2014). UV light activation of TiO$_2$ for sensing formaldehyde: how to be sensitive, recovering fast, and humidity less sensitive. *Sens. Actuators B: Chem.* 202, 964–970. doi: 10.1016/j.snb.2014.06.063

Conflict of Interest Statement: The authors declare that the research was conducted in the absence of any commercial or financial relationships that could be construed as a potential conflict of interest.